3 AIR POLLUTION METEOROLOGY

Most air pollution phenomena occur in the lower part of the atmosphere called the planetary boundary layer, or PBL. The PBL (which is sometimes called the friction layer) is defined as "the region in which the atmosphere experiences surface effects through vertical exchanges of momentum, heat and moisture" (Panofsky and Dutton, 1984).

The traditional approach is to divide the PBL vertically into various layers, each characterized by different "scaling" parameters. Even in ideal conditions (i.e., a horizontally homogeneous and clear PBL) this vertical differentiation by layers is difficult, especially in the "stable" nighttime boundary layer, where, however, some progress in understanding its structure has been made (Nieuwstadt, 1984). The PBL can be divided into three major sublayers:

- The layer near the ground up to the height of the roughness length z_o, whose typical values are presented in Table 3–1. This layer has traditionally been referred to as a "laminar sublayer." Actually, in this layer molecular viscosity hardly plays a role and turbulent fluxes still occur, except very close to the ground (e.g., 1 mm above the ground) where the motion is primarily laminar. This layer, up to the height z_o, could be called the "roughness layer" and defined as the region above the ground in which turbulence is intermittent or not fully developed. (z_o can also be interpreted as the eddy size at the surface.)

- The surface layer (SL) from z_o to h_s, where h_s varies from about 10 m to 200 m. In this layer, the fluxes of momentum, heat and moisture are assumed to be independent of height and the Coriolis effect is generally negligible.

- The transition (or Ekman) layer (TL) from h_s to z_i, where z_i varies from about 100 m to 2 km. The top of the boundary layer z_i is the "lowest level in the atmosphere at which the ground surface no longer influences the dependent variables through the turbulent transfer of mass" (Pielke, 1984). In special situations, such as during thunderstorms, the boundary layer can extend into the stratosphere (an atmospheric layer between about 10 km and 50 km above the ground). Above z_i, turbulence occurs only in shear

Table 3–1. Roughness length z_o of different types of surface (from McRae et al., 1982; numbers in parentheses refer to references in that publication). [Reprinted with permission from Pergamon Press.]

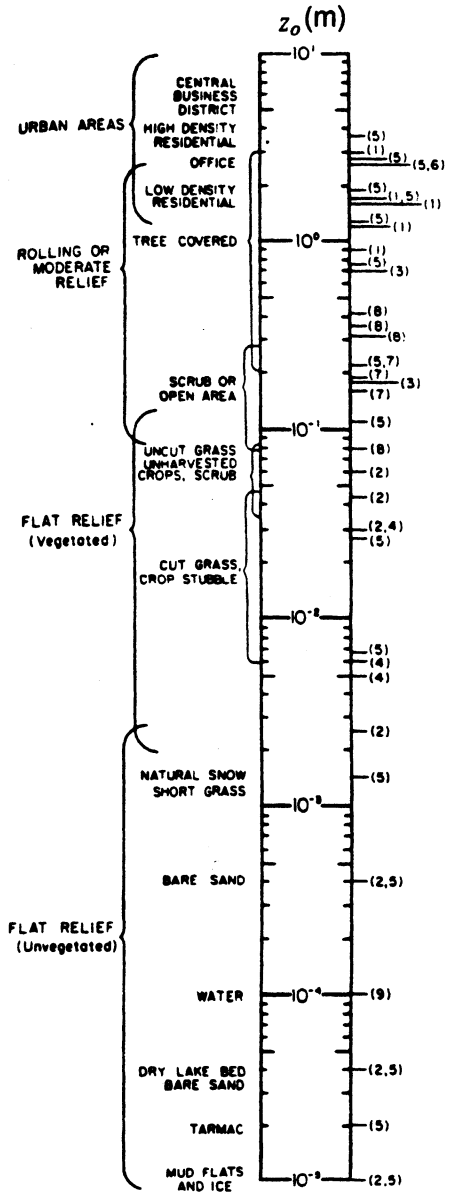

layers (CAT, clear-air turbulence) and inside convective cumulus-type clouds. The altitude z_i is often defined by the height of the lowest temperature inversion, if one exists (Panofsky and Dutton, 1984).

The time-varying meteorological properties of each layer affect the dispersion of pollutants. Between z_o and z_i, turbulent phenomena prevail over molecular phenomena, and the latter become negligible. Below z_o and above z_i, turbulence is not fully developed and therefore molecular motion can play a role in the transfer of mass and energy. Turbulence has strong mixing ability, since its eddies (whose vertical sizes in the atmosphere vary from 1 mm to the size of the PBL) are able to separate nearby parcels of air. As a result, its diffusion rates are several orders of magnitude larger than those of molecular motion.

Among the major meteorological factors that affect air pollution phenomena are

- The horizontal wind (speed and direction), which is generated by the geostrophic wind component, i.e., the pressure gradient wind at the top of the planetary boundary layer (Figure 3-1), and altered by the contribution of terrain frictional forces (Figure 3-2) and the effects of local meteorological winds, such as sea breezes (Figure 3-3), mountain/valley upslope/downslope winds (Figure 3-4) and urban/rural circulations (Figure 3-5)
- The atmospheric stability; i.e., a simple way of categorizing the turbulent status of the atmosphere, which affects the dilution rate of pollutants (Figure 3-6)
- The elevation above the ground
- The strength of the elevated temperature inversion which limits z_i
- The atmospheric vertical motion due to low/high pressure systems (Figure 3-7) or complex terrain effects (hills, mountain ranges, etc.)

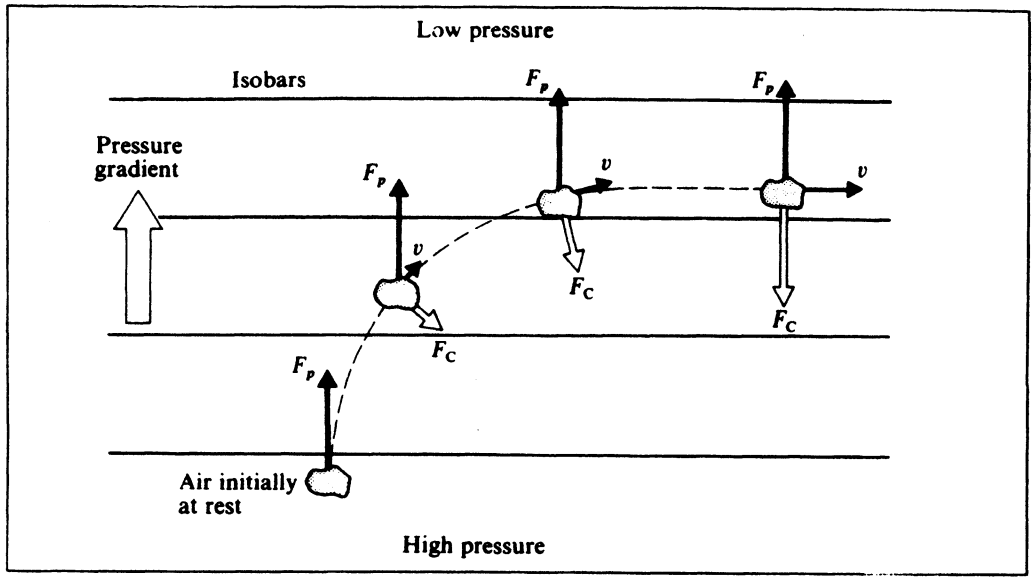

Figure 3–1. Air mass responding to a pressure-gradient force $\mathbf{F_p}$ *is imagined to accelerate initially from rest. Once it gains a velocity* **v**, *the Coriolis force* $\mathbf{F_c}$ *deflects it until a force balance is reached in geostrophic flow (from Williamson, 1973). [Reprinted with permission from Addison–Wesley.]*

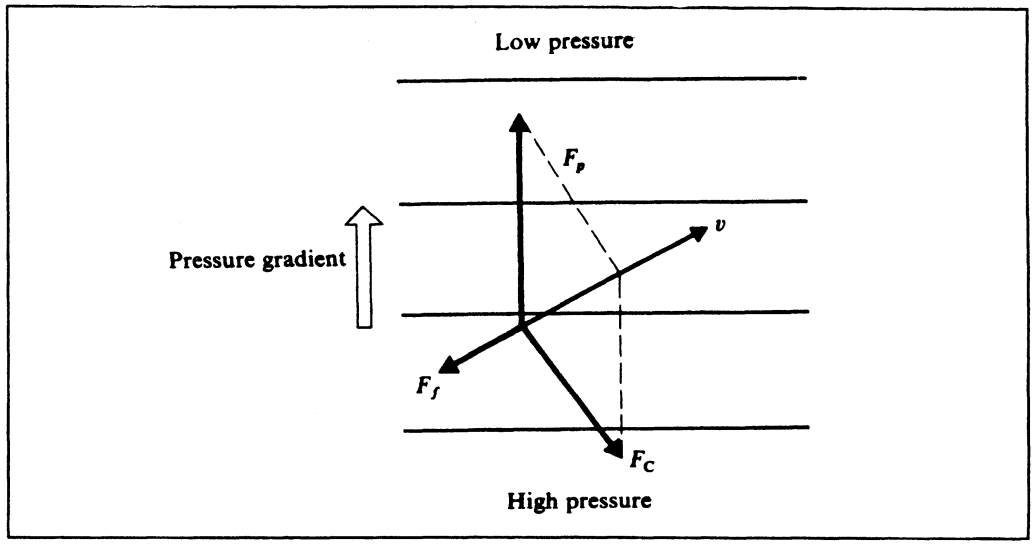

Figure 3–2. Force balance between the pressure gradient force $\mathbf{F_p}$, *the Coriolis force* $\mathbf{F_c}$, *and the frictional force* $\mathbf{F_f}$ *(which must be directed opposite to the wind velocity* **v**) *(from Williamson, 1973). [Reprinted with permission from Addison–Wesley.]*

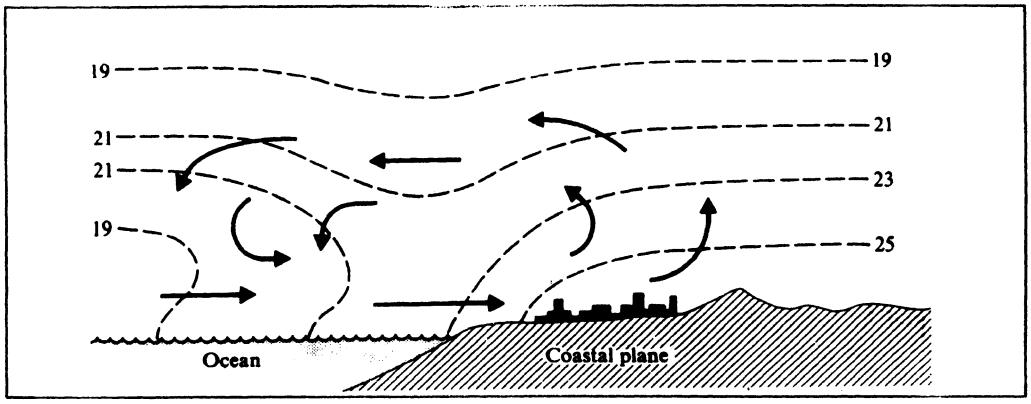

Figure 3–3. *Representative air circulation during a daytime sea breeze. The dashed curves represent contours of uniform temperature (isotherms) and the numbers give their respective temperatures in degrees Celsius (from Williamson, 1973). [Reprinted with permission from Addison–Wesley.]*

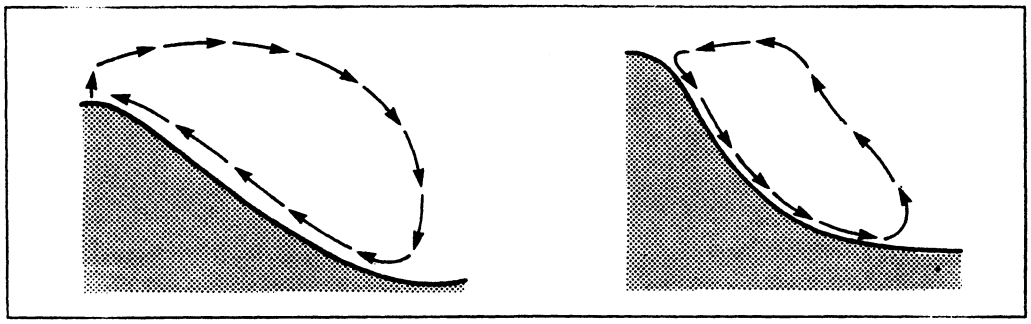

Figure 3–4. *Upslope daytime wind due to greater solar heating on the valley's side than in its center (left), and downslope nighttime wind due to more rapid radiational cooling on the valley's slope than in its center (right). (Adapted from Stern et al., 1984.)[Reprinted with permission from Academic Press.]*

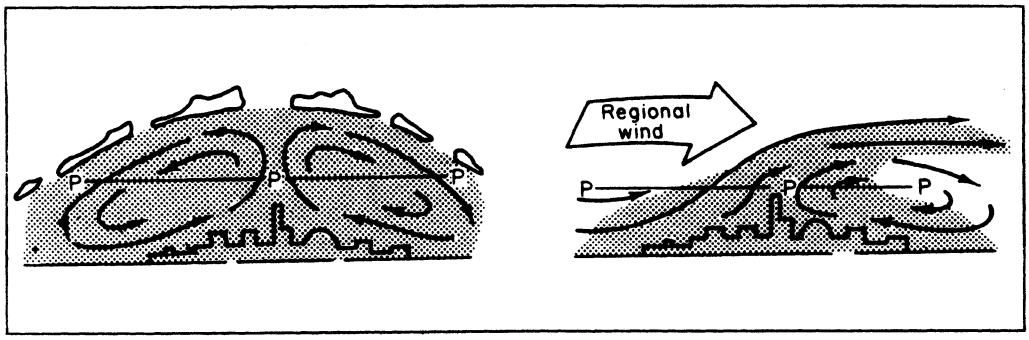

Figure 3–5. *Urban heat island with light regional wind (left) and urban plume with moderate regional wind (right) (from Stern et al., 1984). [Reprinted with permission from Academic Press.]*

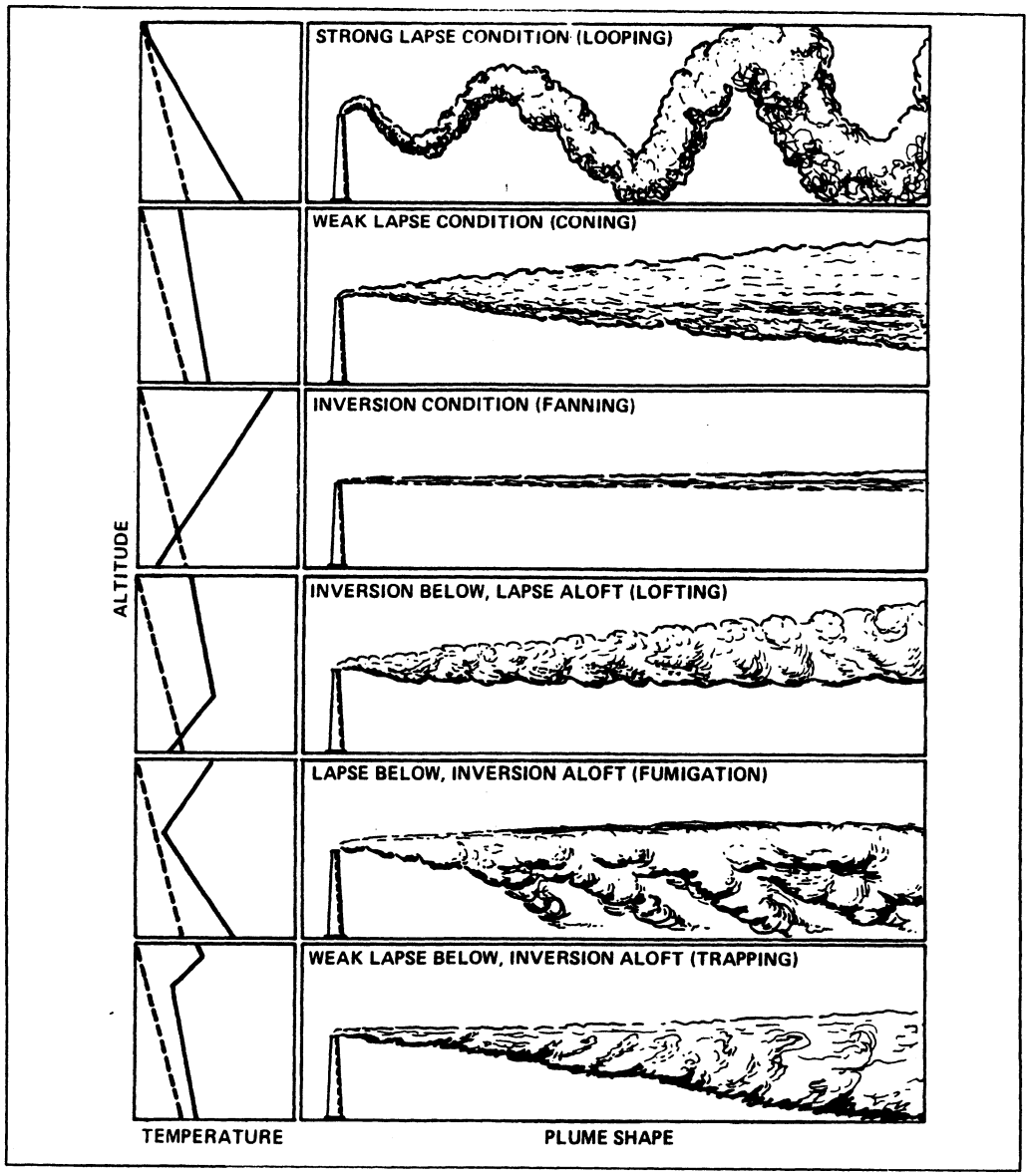

Figure 3–6. Vertical expansion of continuous plumes related to vertical temperature structure. The dashed lines correspond to the dry adiabatic lapse rate for reference (from Stern et al., 1984). [Reprinted with permission from Academic Press.]

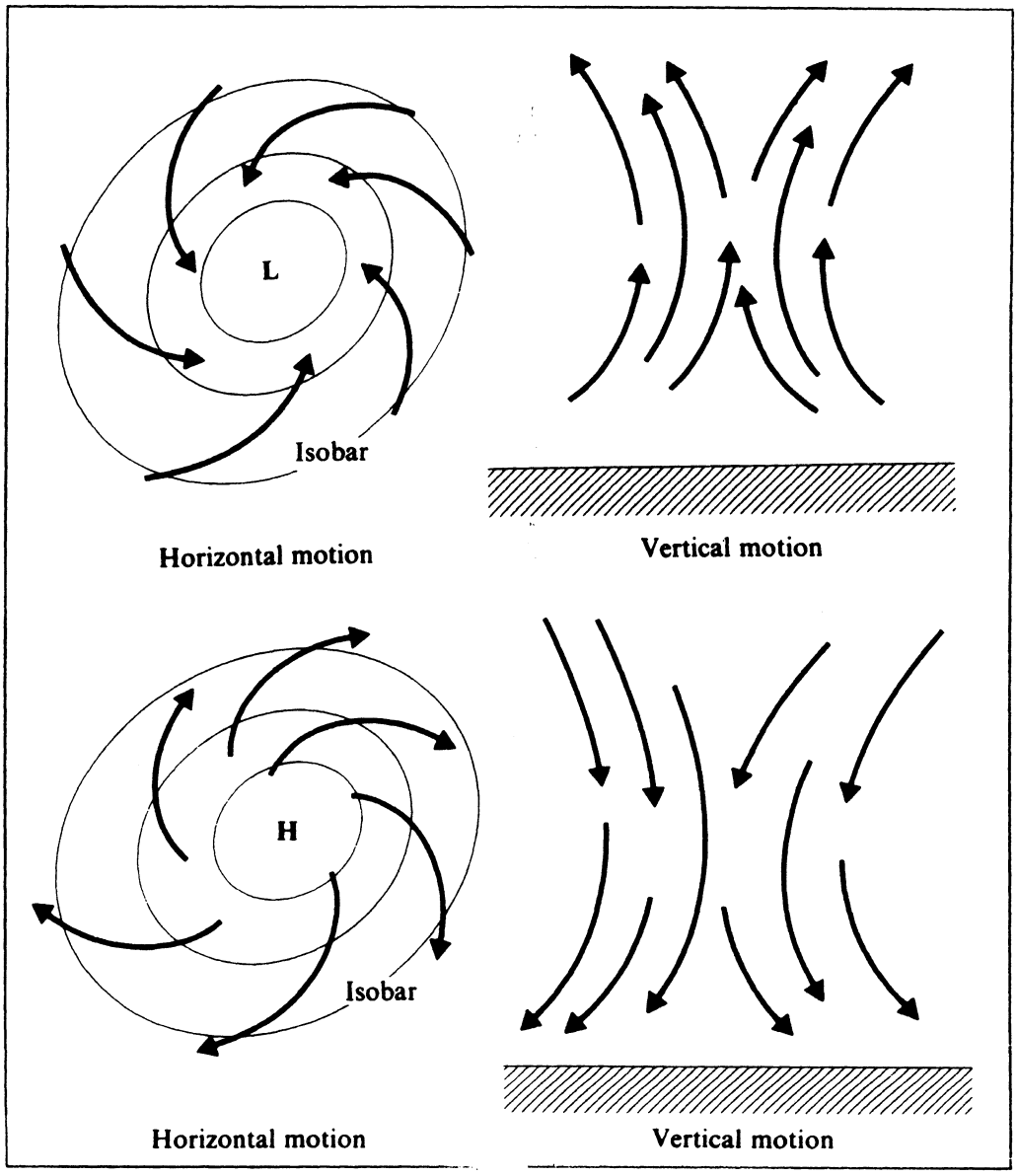

Figure 3–7. *Above: low level counterclockwise spiral of winds, which converge in a cyclone in the Northern Hemisphere; the corresponding vertical motion of the air is depicted at the right. Below: clockwise diverging spiral of winds from an anticyclone in the Northern Hemisphere; the vertically subsiding motion of the air is shown at the right (from Williamson, 1973). [Reprinted with permission from Addison–Wesley.]*

The vertical and, to a lesser extent, horizontal dispersion properties of the PBL are mainly characterized by

- the PBL "stability" conditions (neutral, unstable or stable)
- the PBL's height z_i
- the depth h of the mixed layer (or mixing depth), which is the thickness of the turbulent region next to the ground(*)
- terrain and mesoscale phenomena, with low frequency and directional changes

Atmospheric stability can be characterized by several methods or parameters, such as

- empirical methods (such as the Pasquill scheme presented in Table 3–2 or the Turner method in Table 3–3)
- the flux Richardson number, R_f; i.e., the ratio of the rate of dissipation (or production) of turbulence by buoyancy to the rate of creation of turbulence by shear ($R_f < 0$ for unstable conditions, = 0 for neutral, and > 0 for stable); the absolute value of R_f also indicates the relative importance of convective to mechanical turbulence
- the gradient Richardson number, R_i (related to R_f but easier to measure)
- the Monin–Obukhov length, L ($1/L < 0$ for unstable conditions, $\simeq 0$ for neutral, and > 0 for stable)

3.1 NEUTRAL CONDITIONS

Neutral conditions are characterized by the presence of an isentropic (or adiabatic) vertical temperature profile in the PBL (i.e., $\Delta T/\Delta z \simeq 9.86 \cdot 10^{-3}$ deg/m in dry air, where T is the temperature and z the altitude). They typically occur during daytime–nightime transitions, cloud overcasts, or with strong winds (e.g., greater than 6 m/s at a 10–m elevation, where 10 m is the standard elevation recommended for surface wind monitoring).

(*) In neutral and unstable conditions, $z_i \simeq h$, while in stable conditions, where z_i is the thickness of the ground–based temperature inversion, $h < z_i$, as discussed further below.

Table 3–2. Pasquill dispersion classes: A, very unstable; B, unstable; C, slightly unstable; D, neutral; E, slightly unstable; F, stable; G, very stable (from Dobbins, 1979; adapted from Pasquill, 1974). [Reprinted with permission from John Wiley and Sons.]

Insolation/Cloud Cover		Surface Wind Speed (m/s)				
		<2.0	2 to <3	3 to <5	5 to <6	≥6
Day	Strong Insolation	A	A–B	B	C	C
	Moderate Insolation	A–B	B	B–C	C–D	D
	Slight Insolation	B	C	C	D	D
Day or Night	Overcast	D	D	D	D	D
Night	Thin overcast or ≥0.5 cloud cover	—	E	D	D	D
	≤0.4 cloud cover	—	F	E	D	D

Notes: 1. Strong insolation corresponds to a solar elevation angle of 60° or more above the horizon. Slight insolation corresponds to a solar elevation angle of 15° to 35°.

2. Pollutants emitted under clear nighttime skies with winds less than 2.0 m/s, more recently defined to be class G, may be subject to unsteady meandering which renders the prediction of concentrations at downwind locations unreliable.

Table 3–3. Definition of Turner Classes: 1, very unstable; 2, unstable; 3, slightly unstable; 4, neutral; 5, slightly stable; 6, stable; 7, very stable (from Panofsky and Dutton, 1984). [Reprinted with permission from John Wiley and Sons.]

Wind Speed (knots)	Net Radiation Index						
	4	3	2	1	0	−1	−2
0–1	1	1	2	3	4	6	7
2–3	1	2	2	3	4	6	7
4–5	1	2	3	4	4	5	5
6	2	2	3	4	4	5	6
7	2	2	3	4	4	4	5
8–9	2	3	3	4	4	4	5
10	3	3	4	4	4	4	5
11	3	3	4	4	4	4	4
≥ 12	3	4	4	4	4	4	4

Solar Altitude (a)	Insolation	Insolation Class Number
$60° < a$	Strong	4
$35° < a < 60°$	Moderate	3
$15° < a < 35°$	Weak	2
$a \leq 15°$	Very Weak	1

DEFINITIONS OF NET RADIATION INDEX

1. If the total cloud cover is 10/10 and the ceiling is less than 7000 ft, use net radiation index equal to 0 (whether day or night).
2. For nighttime (between sunset and sunrise):
   (a) If total cloud cover ≤ 4/10, use net radiation index equal to −2.
   (b) If total cloud cover > 4/10, use net radiation index equal to −1.
3. For daytime:
   (a) Determine the insolation class number as a function of solar altitude from Table 6.4.
   (b) If total cloud cover ≤ 5/10, set the net radiation index above equal to the insolation class number.
   (c) If cloud cover > 5/10, modify the insolation class number by the following six steps.
      (1) Ceiling < 7000 ft, subtract 2.
      (2) Ceiling ≥ 7000 ft but < 16,000 ft, subtract 1.
      (3) Total cloud cover equals 10/10, subtract 1. (This will only apply to ceilings ≥ 7000 ft since cases with 10/10 coverage below 7000 ft are considered in item 1 above.)
      (4) If insolation class number has not been modified by steps (1), (2), or (3) above, assume modified class number equal to insolation class number.
      (5) If modified insolation class number is less than 1, let it equal 1.
      (6) Use the net radiation index in Table 6.4 corresponding to the modified insolation class number.

Since urban areas do not become as stable in the lower layers as nonurban areas, stability classes computed as 6 and 7 by this system are called class 5 in urban areas.

In neutral conditions (Panofsky and Dutton, 1984), the PBL's height is estimated (when no measurements of an elevated inversion are available) by

$$z_i \simeq h = const \frac{u_*}{f} \tag{3-1}$$

where *const* = 0.15 to 0.25 and the friction velocity u_* and the Coriolis parameter f are

$$u_* = (-\overline{u' w'})^{1/2} = \sqrt{\tau(0)/\varrho} \tag{3-2}$$

$$f = 2\,\Omega\,\sin\phi \tag{3-3}$$

where u' and w' are the surface wind velocity fluctuations parallel to the mean horizontal wind and vertical, respectively; $\tau(0)$ is the surface stress (also called the downward flux of momentum along the main wind direction); ϱ is the air density; Ω is the earth's rate of rotation ($7.29 \cdot 10^{-5}\ s^{-1}$); and ϕ is the latitude. The surface stress $\tau(0)$ is the ground-level value of the modulus of the horizontal Reynolds stress tensor $\boldsymbol{\tau}$, which, according to the K-theory (in which the flux is assumed to be proportional to the gradient), can be formulated as

$$\boldsymbol{\tau}(z) = K_m \varrho \frac{\partial \mathbf{u}}{\partial z} \tag{3-4}$$

where K_m is the scalar eddy viscosity and $\mathbf{u}$ is the average horizontal wind vector.

Experimental studies show, however, that the actual z_i is often lower than the value predicted by Equation 3-1, since large-scale processes (e.g., air subsidence during high-pressure situation) produce an elevated inversion layer whose bottom elevation represents the actual z_i.

3.2 UNSTABLE CONDITIONS

Unstable conditions are typical in the daytime with positive heat flux at the ground (i.e., sunny conditions). In these conditions, h tends to be about 10 percent higher than the height of the bottom of the lowest elevated inversion, since the lowest part of the inversion layer is often moderately turbulent due to penetrating eddies from below and wind shear effects.

When the height of the lowest elevated inversion is not known, a simple equation for the daily time-variation of $h(t)$ can be derived from the heat energy budget. In fact (Panofsky and Dutton, 1984), it is

$$\gamma_d - \gamma = \frac{\Delta T_o}{h(t)} \tag{3-5}$$

where γ_d is the dry adiabatic lapse rate ($\gamma_d = 9.86\ 10^{-3}$ °C/m), γ is the atmospheric lapse rate (i.e., $\gamma = -\partial T/\partial z$) at sunrise, and ΔT_o is the surface temperature increase between the time t_o (sunrise) and t. Also, conservation of heat energy gives

$$\int_{t_o}^{t} H\,dt = \frac{c_p\,\varrho\,h(t)\,\Delta T_o}{2} \tag{3-6}$$

where H is the surface heat flux, c_p is the specific heat at constant pressure (about 1,000 J deg^{-1} kg^{-1} for dry air), and ϱ is the air density. By combining Equations 3-5 and 3-6, we obtain

$$h(t) = \left(\frac{2 \int_{t_o}^{t} H\,dt}{c_p\,\varrho\,(\gamma_d - \gamma)} \right)^{1/2} \tag{3-7}$$

which can be solved analytically or numerically if $H(t)$ is specified.

In unstable conditions, R_f, R_i and L are negative and $-L$ is the height that separates mainly mechanical turbulence below from mainly convective turbulence above.

3.3 STABLE CONDITIONS

Stable conditions are typically encountered over land during clear nights with weak winds. Under these conditions, a ground-based temperature inversion is present and the temperature increases with height from $z = 0$ to $z = z_i$, the top of the stable PBL. Mechanical turbulence, however, even though strongly attenuated by the downward heat flux H ($H < 0$), creates a mixing layer from $z = 0$ to $z = h$, where h can be much lower than z_i. Monitoring by acoustic sounding techniques is very useful for evaluating h under these conditions. If these measurements are not available, the steady-state asymptotic value h_{eq} of $h(t)$ can be

computed by the formula suggested by Zilitinkevich (see Businger and Arya, 1974).

$$h_{eq} = const \sqrt{\frac{u_*}{f} L} \tag{3-8}$$

with $const \simeq 0.4$ (Garratt, 1982).

Nighttime conditions are frequently characterized by multiple stable layers aloft. This situation is difficult to parameterize, especially because the motion in each layer is almost independent and large wind shear effects are, therefore, encountered. Moreover, real equilibrium conditions are seldom found, which further limits the applicability of Equation 3-8.

3.4 THE STRATIFICATION OF THE PBL

Recent studies have identified new intricacies in the regional differentiation of the PBL, whose vertical structure is more complex than the simple three-layer separation discussed at the beginning of this chapter. Holtslag and Nieuwstadt (1986) provided a detailed discussion on the different scaling regions of the PBL, a discussion which is summarized in Figure 3-8. The main layers shown in Figure 3-8 are discussed further below.

3.4.1 The Surface Layer

The vertical fluxes of heat and momentum in the PBL are typically large at the surface and decrease to zero at z_i. The lower part of the PBL is called the surface layer (or constant-stress layer) and is defined as that layer above the ground in which the vertical variation of the heat and momentum fluxes is negligible (e.g., less than 10 percent). Panofsky and Dutton (1984) suggest that the depth of the surface layer h_s is

$$h_s \simeq h/10 \tag{3-9}$$

which gives $h_s \simeq 100$ m in typical daytime unstable conditions (with $h \simeq 1{,}000$ m) and $h_s \leq 10$ m with typical nighttime stable conditions (where $z_i \simeq 300$ m, but $h \leq 100$ m).

In the surface layer, since τ does not vary with z, the wind direction is constant (see Equation 3-4). Moreover, in the surface layer, the earth's rotation

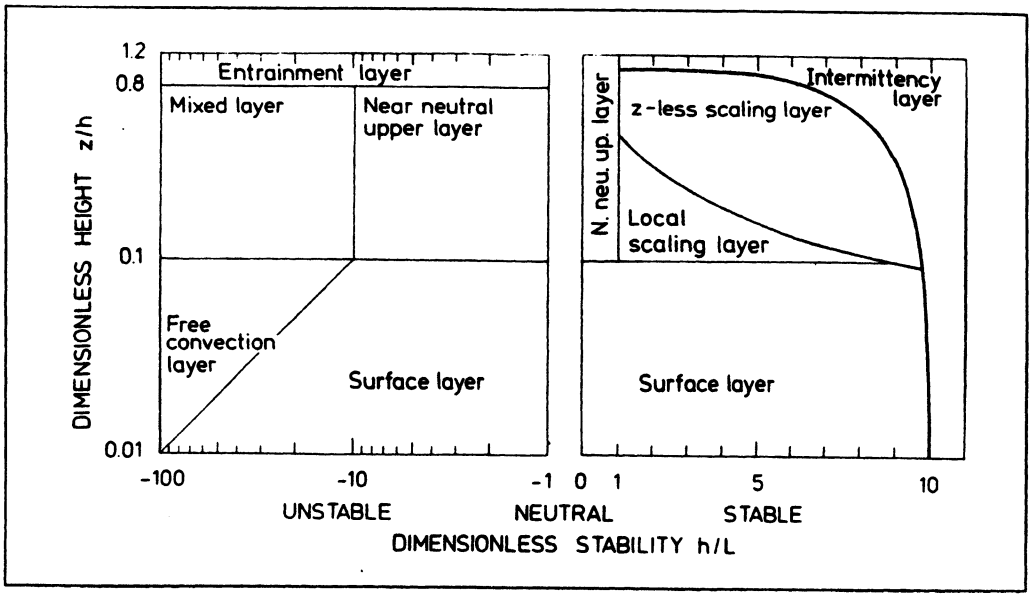

Figure 3–8. The scaling regions of the atmospheric boundary layer, shown as function of the dimensionless height z/h and the stability parameter h/L. When used to determine dispersion regions, the dimensionless height is replaced by z_s/h where z_s is the source height (from Gryning et al., 1987, adapted from Holtslag and Nieuwstadt, 1986). [Reprinted with permission from Pergamon Press.]

effects are assumed to be negligible. Surface layer meteorology and dispersion rates have been satisfactorily explained by the similarity theory, which was first developed by Monin and Obukhov (1954) and which is discussed in Section 3.6. The advantage of this theory is that several atmospheric parameters, when normalized using u_* and L, show a universal behavior that is a function only of z/L.

3.4.2 The Mixed Layer

During unstable conditions, most of the PBL (from $z = -L$ to $z = z_i$) is characterized by dominant convective conditions that require a different scaling from the one provided by the surface layer similarity theory (which is only valid for $z \leq 0.1\ z_i$). This was provided by the mixed-layer scaling introduced by Deardorff (1970), which uses z_i as a length scale (instead of $|L|$), a new velocity

scale w_* instead of u_*, and a third scale, the temperature scale θ_*. They are defined by

$$w_* = \left(\frac{g\,H\,z_i}{c_p\,\varrho\,T_o}\right)^{1/3} \tag{3-10}$$

where g is the acceleration due to gravity (9.806 m s^{-2}), T_o is the surface temperature, and

$$\theta_* = -\frac{H}{c_p\,\varrho\,w_*} \tag{3-11}$$

3.4.3 The Free Convection Layer

During unstable conditions, when z_i is large enough, there is a region in which both surface layer similarity and mixed-layer scaling are valid. This layer, $-L < z < 0.1\ z_i$, when present, is called the free convection layer.

3.4.4 The Stable Layer

A stable atmospheric boundary layer is common over land at night. Under these conditions, h can vary from a few tens of meters with light winds to several hundred meters with strong winds. Caughey et al. (1979) have proposed a stable layer scaling using h as the length scale (as in the mixed layer) and u_* as a velocity scale (as in the similarity theory, since stable layer turbulence is mechanical and not convective).

Theoretical and experimental studies in the stable layer are complicated by the fact that the nighttime boundary layer is usually not in equilibrium, and by the effects of gravity waves (Panofsky and Dutton, 1984). A new "local scaling" approach (Nieuwstadt, 1984) for the stable atmospheric boundary layer, which uses a local (i.e., variable with z) Obukhov length Λ, is discussed in Section 3.7.

3.4.5 The Entrainment Interfacial Layer

Special studies and parameterizations of the entrainment interfacial layer, defined as the layer between approximately 0.8 z_i and 1.2 z_i, have been performed by Deardorff (1972), by Wyngaard et al. (1974) and, more recently and comprehensively, by Wyngaard and LeMone (1980).

3.5 SEMIEMPIRICAL ESTIMATES OF BOUNDARY LAYER PARAMETERS

Meteorological measurements of boundary layer parameters are not often available and, therefore, in most cases, the PBL parameters are not measured directly but inferred from standard meteorological information available for the study region.(*) In this section, semiempirical numerical methods and formulations that allow estimation of PBL parameters are presented.

3.5.1 The PBL Height z_i

The value z_i is determined by the top of the ground-based nighttime inversion (in stable conditions) or the bottom of the first elevated inversion (unstable conditions). In neutral conditions, z_i can be computed by Equation 3–1, unless an elevated inversion is lower than this computed value (in which case z_i is the bottom of the elevated inversion). In unstable conditions, z_i can be computed by Equations 3–6 and 3–7. In stable conditions, z_i can be approximated, at mid-latitudes, by the value $2.4 \cdot 10^3 \, u_*^{3/2}$ (Venkatram, 1980).

3.5.2 The Mixing Height h

In neutral or unstable conditions, the mixing height h is $\simeq z_i$ (or, according to some, 10 percent greater than z_i). In stable conditions, h can be approximated by Equation 3–8.

3.5.3 The Roughness Length z_o

The parameter z_o is generally a function of surface roughness only, even though it may be affected by the wind speed (when the roughness elements bend with the wind) and wind direction (when different terrain features surround the region). It has also been suggested that an "effective" value of z_o should increase with height (Wilczak and Phillips, 1986). The value of z_o can be obtained from tables such as Table 3–1 or computed approximately as

$$z_o = \epsilon/30 \tag{3–12}$$

where ϵ is the average height of the obstacles in the study area.

The roughness length can also be computed from wind profile measurements. In fact, in purely mechanical turbulence (i.e., with strong winds), the

(*) See van Ulden and Holtslag (1985) for an outline of a meteorological preprocessor that is capable of calculating the major PBL parameters that affect atmospheric dispersion from routinely available measurements (and other special measurements, if available).

average wind speed u shows a classical logarithmic wind profile for $z > z_o$, which is given by

$$u(z) = \frac{u_*}{k} \ln\left(\frac{z}{z_o}\right) \tag{3-13}$$

where k is the von Karman constant ($\simeq 0.40$). Equation 3–13 is valid only for uniform terrain. Even in nonuniform terrain, though, Equation 3–13 can be used for representing the average u over large horizontal areas (Panofsky and Dutton, 1984). When the height of the large roughness elements (such as buildings and vegetation) is much smaller than the height of wind observations, Equation 3–13 provides an immediate solution for z_o, using two wind speed measurements u_1 and u_2 at different elevations z_1 and z_2, respectively:

$$\frac{u_2}{u_1} = \frac{\ln\ (z_2/z_o)}{\ln\ (z_1/z_o)} \tag{3-14}$$

When the roughness elements are not small, a displacement length d can be defined (Panofsky and Dutton, 1984), which is typically 70 to 80 percent of the height of the large roughness elements. In this case (see Figure 3–9), the wind profile will be (for $z > d$)

$$u(z) = \frac{u_*}{k} \ln\left(\frac{z-d}{z_o}\right) \tag{3-15}$$

which, again, allows the evaluation of z_o from

$$\frac{u_2}{u_1} = \frac{\ln[(z_2-d)/z_o]}{\ln[(z_1-d)/z_o]} \tag{3-16}$$

3.5.4 The Friction Velocity u_*

During strong winds, the friction velocity u_* can be computed from Equations 3–13 or 3–15 using z_o and a single wind measurement $u_1 = u(z_1)$.

3.5.5 The Surface Stress $\tau(0)$

The surface stress $\tau(0)$ can be estimated by Equation 3–2 using u_*.

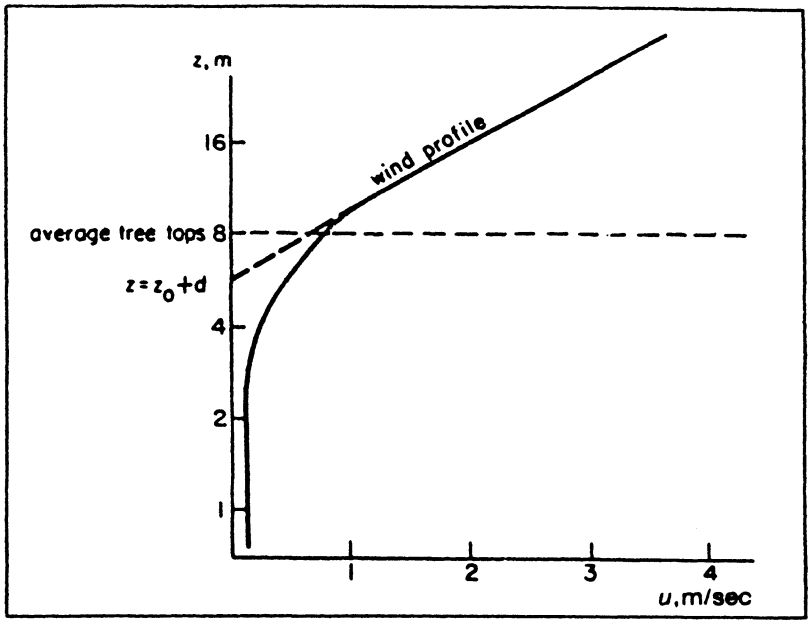

Figure 3–9. Example of wind profile above large roughness elements such as tree (from Panofsky and Dutton, 1984). [Reprinted with permission from John Wiley and Sons.]

3.5.6 K_m in the Neutral Surface Layer

From Equations 3–4 and 3–13, remembering the $\tau(z)$ is constant in t surface layer, the eddy viscosity K_m can be estimated in neutral conditions from single wind measurement by

$$K_m = \frac{k^2 u_1 z_1}{\ln(z_1/z_o)} \qquad (3\text{–}1$$

3.5.7 Monin–Obukhov Length L

The Monin–Obukhov length L is a parameter that characterizes the "s bility" of the surface layer and is calculated from ground-level measurements is computed from

$$L = -\frac{u_*^3 c_p \varrho T}{k g H (1 + 0.07/B)} = -\frac{u_*^3 z_i}{k w_*^3 (1 + 0.07/B)} \simeq -\frac{z_i}{k}\left(\frac{u_*}{w_*}\right)^3 \qquad (3\text{–}1$$

where B is the Bowen ratio (i.e., the ratio of sensible to latent(*) surface heat flux), which can be estimated by

$$B = \frac{\Delta T + 0.01\ \Delta z}{2500\ \Delta q} \tag{3-19}$$

where $\Delta T/\Delta z$ is the temperature vertical gradient and $\Delta q/\Delta z$ is the specific vertical humidity gradient (both at the surface).

L can also be estimated empirically as a function of the Turner class (see Table 3-3) and z_o, as illustrated in Figure 3-10. The empirical curves in Figure 3-10 have been analytically fitted by Liu et al. (1976) and Irwin (1979) using power law functions such as $1/L = a\, z_o^b$. Table 3-4 provides the values of the constants a and b.

Venkatram (1980) has proposed another empirical formulation for L (only for stable nighttime conditions). It is

$$L = 1.1\ 10^3\ u_*^2 \tag{3-20}$$

3.5.8 The Surface Heat Flux H

The surface heat flux H is defined as

$$H = c_p\ \varrho\ \overline{w'T'} \tag{3-21}$$

where w' and T' are the surface values of the fluctuating components of the vertical wind and temperature, respectively. Using the gradient-theory (or K-theory), in which the heat flux is proportional to the temperature gradient, we obtain

$$H(z) = -K_h\, c_p\, \varrho \left(\frac{\partial T}{\partial z} + \gamma_d\right) \tag{3-22}$$

(*) The sensible heat flux is generally proportional to the vertical temperature gradient, while the latent heat flux is the enthalpy flux of water vapor.

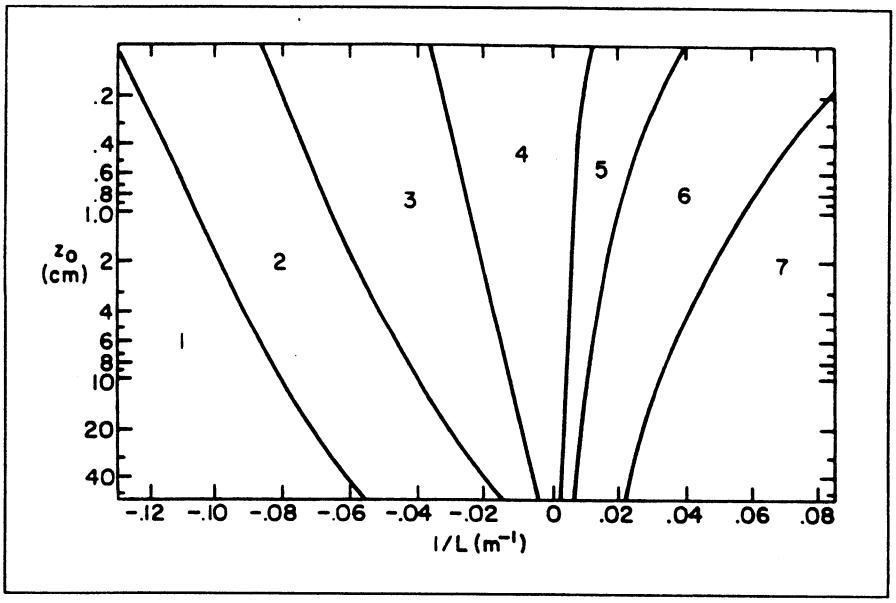

Figure 3–10. Semiempirical relation between L, the Turner class and z_o (from Golder, 1972, as presented by Panofsky and Dutton, 1984). [Reprinted with permission from John Wiley and Sons.]

Table 3–4. Coefficient a, b for the fitting of the curves in Figure 3–10 by $(1/L) = a\, z_o^b$.

Stability Class	*a*	*b*
A	-0.0875	-0.1029
B	-0.03849	-0.1714
C	-0.00807	-0.3049
D	0.	0.
E	0.00807	-0.3049
F	0.03849	-0.1714

which allows an estimate of H at z_o using surface values of ϱ and $\partial T/\partial z$ (K_h is the coefficient of eddy heat conduction). Equation 3–22 can be rewritten as

$$H = -K_h c_p \varrho \left(\frac{\partial \theta}{\partial z}\right)_{z=o} \tag{3–23}$$

using the potential temperature θ defined by

$$\theta(z) = T(z) + \gamma_d z \tag{3–24}$$

3.5.9 The Velocity Scale w_* in the Mixed Layer

The convective velocity scale w_* is computed by

$$w_* = \left(\frac{g H z_i}{c_p \varrho T_0}\right)^{1/3} \tag{3–25}$$

3.5.10 The Temperature Scale θ_* in the Mixed Layer

The temperature scale θ_* is computed by

$$\theta_* = -\frac{H}{c_p \varrho w_*} \tag{3–26}$$

3.5.11 The Richardson Numbers

The Richardson numbers are useful parameters for evaluating atmospheric stability (stable, neutral and unstable conditions correspond to positive, zero and negative Richardson numbers, respectively).

An approximate estimate of the gradient Richardson number R_i can be obtained (Businger, 1966; Pandolfo, 1966) by

$$R_i = z/L \tag{3–27}$$

in unstable conditions and

$$R_i = \frac{z/L}{1 + 5\, z/L} \tag{3-28}$$

in stable conditions.

A quantity easier to measure than R_i, is the bulk Richardson number R_b, given by

$$R_b = \frac{g\, z}{T} \frac{\frac{\partial T}{\partial z} + \gamma_d}{u^2} \tag{3-29}$$

which is related to R_i by

$$R_i = \frac{R_b}{r^2} \tag{3-30}$$

where r is the exponent of the power law

$$u(z) = u_1 \left(\frac{z}{z_1}\right)^r \tag{3-31}$$

that best fits the wind profile. (The level z_1 is arbitrary.) A typical value of r in flat terrain is 1/7, while in rough terrain r can be more than twice this value.

Finally, the relation between the flux Richardson number, R_f, and R_i is

$$R_f = \frac{K_h}{K_m} R_i \tag{3-32}$$

3.5.12 The Variances of Wind Components

In standard meteorological notation (u parallel to the mean wind, v the horizontal crosswind component, and w the vertical component) the horizontal and vertical wind fluctuations are characterized by their "intensities" σ_u, σ_v, σ_w; i.e., the standard deviations of the instantaneous u, v, *and* w values, respectively.

In neutral conditions, it can be assumed that

$$\sigma_u = a\, u_* \tag{3-33}$$

$$\sigma_v = b\, u_* \tag{3-34}$$

$$\sigma_w = c\, u_* \tag{3-35}$$

with the following estimates of the constants in flat terrain (Panofsky and Dutton, 1984)

$$a = 2.39 \pm 0.03 \tag{3-36}$$

$$b = 1.92 \pm 0.05 \tag{3-37}$$

$$c = 1.25 \pm 0.03 \tag{3-38}$$

In rolling terrain, a and b are larger, but c does not seem to change.

In the unstable surface layer, Panofsky et al. (1977a) recommend

$$\sigma_w(z) = 1.25\, u_* \left(1 - 3\frac{z}{L}\right)^{1/3} \tag{3-39}$$

which seems to work in both flat and rolling terrain. For large z in unstable conditions, σ_w becomes independent of u_*. The limit of Equation 3-39 for large z gives

$$\sigma_w(z) = 1.3 \left(\frac{g\, H\, z}{c_p\, \varrho\, T}\right) \tag{3-40}$$

which fits several observations well.

In the entire PBL under unstable conditions, Wilczak and Phillips (1986) obtained

$$\frac{\sigma_w}{w_*} = \left\{1.8\, (z/z_i)^{2/3}\, [1 - 0.91\, (z/z_i)]\right\}^{1/2} \tag{3-41}$$

which fits well both the measurements of Caughey and Palmer (1979) and the laboratory experiments by Deardorff (1974). However, when they compare Equation 3-41 with another set of data (26 days of data collected in the late summers of 1982 and 1983 at the Boulder Atmospheric Observatory, BAO), they obtain σ_w values that are too small (about 20 percent) in magnitude and that can

be fitted, instead, by substituting the constant 2.5 for the constant 1.8 in Equation 3-41.

In the surface layer, Panofsky et al. (1977b) suggest

$$\sigma_u = \sigma_v = u_* \left(12 - 0.5 \frac{z_i}{L}\right)^{1/3} \tag{3-42}$$

for stable and unstable (but not neutral) conditions.

In the entire PBL under unstable conditions, Wilczak and Phillips (1986) suggest

$$\frac{\sigma_u}{w_*} = \frac{\sigma_v}{w_*} = c \left\{ 0.5 \left[2 - (z/z_i)^{1/2}\right] + 0.3 (z/z_i)^{1/2} \right\}^{1/2} \tag{3-43}$$

where c is the surface value ($z = 0$) of σ_u/w_* or σ_v/w_* (a typical value is $c = 0.74$).

3.5.13 Best Fit Estimates of PBL Parameters

Numerical algorithms have been developed that provide best fit estimates of PBL parameters from a limited set of measurements. Similarity theory equations are generally used for these computations.

Nieuwstadt (1978) provided a numerical iterative method that, using average wind $u(z)$ and temperature $\theta(z)$ profiles, minimizes the difference between measurements and theoretical values. This minimization gives a solution for θ_*, u_*, and, therefore, L. The method works better when z_o is known. A second method by Aloysius (1979) is, at least in theory, more powerful, since it allows the evaluation of practically all PBL parameters (L, z_o, u_*, θ_*, H, R_i) using a single profile of either wind or temperature. Both methods have been successfully compared with field measurements.

3.6 SCALING IN THE SURFACE LAYER

The similarity theory (Monin and Obukhov, 1954) allows a valid parameterization of the surface layer. According to this theory (Panofsky and Dutton,

1984), the nondimensional wind shear $\phi_m(z/L)$ is defined by

$$\phi_m(z/L) = \frac{k\,z}{u_*}\,\frac{\partial u}{\partial z} \tag{3-44}$$

where, in neutral conditions,

$$\phi_m = 1 \tag{3-45}$$

in unstable conditions

$$\phi_m = (1 - 16\,z/L)^{-1/4} \tag{3-46}$$

or

$$\phi_m = (1 - 15\,z/L)^{-1/3} \tag{3-47}$$

or

$$\phi_m^4 - 15\,(z/L)\,\phi_m^3 = 1 \tag{3-48}$$

and in stable conditions

$$\phi_m = 1 + 5\,z/L \tag{3-49}$$

The average wind speed u can be obtained by integrating Equation 3-44, a process that does not require the knowledge of the exact form of ϕ_m. It is

$$u(z) = (u_*/k)[\ln(z/z_o) - \psi_m(z/L)] \tag{3-50}$$

where ψ_m is the universal function in the diabatic surface layer wind profile

$$\psi_m(z/L) = \int_{z_o/L}^{z/L} [1 - \phi_m(\zeta)]\frac{d\zeta}{\zeta} \tag{3-51}$$

In neutral conditions

$$\psi_m = 0 \tag{3-52}$$

while, in unstable conditions,

$$\psi_m \simeq \ln\left[\left(\frac{1+x^2}{2}\right)\left(\frac{1+x}{2}\right)^2\right] - 2\,arctg\,x + \pi/2 \qquad (3\text{–}53)$$

with $x = (1 - 16\,z/L)^{1/4}$, and in stable conditions

$$\psi_m = -5\,z/L \qquad (3\text{–}54)$$

In an analogous way, the nondimensional temperature gradient $\phi_h(z/L)$ is defined as

$$\phi_h = \frac{k\,z}{T_*}\,\frac{\partial\theta}{\partial z} \qquad (3\text{–}55)$$

where θ is the potential temperature defined by Equation 3–24 and T_* is the temperature scaling parameter

$$T_* = -\frac{H}{c_p\,\varrho\,u_*} \qquad (3\text{–}56)$$

In neutral conditions

$$\phi_h = 1 \qquad (3\text{–}57)$$

while in unstable conditions

$$\phi_h = (1 - 16\,z/L)^{-1/2} \qquad (3\text{–}58)$$

or

$$\phi_h = 0.74\,(1 - 9\,z/L)^{-1/2} \qquad (3\text{–}59)$$

and in stable conditions

$$\phi_h = 1 + 5\,z/L \qquad (3\text{–}60)$$

or

$$\phi_h = 0.74 + 4.7\,z/L \qquad (3\text{–}61)$$

Again, the integration of Equation 3–55 gives the value of θ at a certain

elevation z, i.e.,

$$\theta(z) - \theta(z_o) = (T_* / k) [\ln(z/z_o) - \psi_h(z/L)] \tag{3-62}$$

where

$$\psi_h(z/L) = \int_{z_o/L}^{z/L} [1 - \phi_h(\zeta)] \frac{d\zeta}{\zeta} \tag{3-63}$$

is the universal function in diabatic surface layer temperature profile.

In neutral conditions

$$\psi_h = 0 \tag{3-64}$$

while in unstable conditions

$$\psi_h \simeq 2 \ln\left[0.5 \left(1 + \sqrt{1 - 16\, z/L}\right)\right] \tag{3-65}$$

and in stable conditions

$$\psi_h = -5\, z/L \tag{3-66}$$

The same concepts apply to other scalars; e.g., the specific humidity q. We just replace $c_p T$ with q and obtain

$$q(z) - q(z_o) = (q_*/k)[\ln(z/z_o) - \psi_q(z/L)] \tag{3-67}$$

where the scaling parameter for the scalar q is

$$q_* = -\frac{Q}{u_* \varrho} \tag{3-68}$$

which is analogous to Equation 3-56, using the vertical flux Q of the scalar q instead of the heat flux H. It is still not clear how to define ψ_q. At present, it seems best to assume $\psi_q = \psi_h$ (Panofsky and Dutton, 1984).

The standard deviation of the vertical wind velocity can be scaled by

$$\sigma_w / u_* = \phi_3(z/L) \tag{3-69}$$

In neutral conditions

$$\phi_3 = const = 1.25 \pm 0.03 \tag{3-70}$$

and in unstable conditions

$$\phi_3 \simeq 1.25\ (1 - 3\ z/L)^{1/3} \tag{3-71}$$

while in stable conditions the large scatter of the data points has not yet allowed a clear interpolation.

The standard deviations of the horizontal wind velocity are scaled by

$$\sigma_u/u_* = \phi_1(z_i/L) \tag{3-72}$$

$$\sigma_v/u_* = \phi_2(z_i/L) \tag{3-73}$$

and are independent of height. In neutral conditions they are constant

$$\phi_1 = 2.39 \pm 0.03 \tag{3-74}$$

$$\phi_2 = 1.92 \pm 0.05 \tag{3-75}$$

while in stable or unstable conditions (Panofsky et al., 1977a) they vary with z_i/L, i.e.,

$$\phi_1 \simeq \phi_2 \simeq (12 - 0.5\ z_i/L)^{1/3} \tag{3-76}$$

The standard deviation of a scalar (e.g., q) is scaled by

$$\sigma_q/q_* = \phi_Q(z/L) \tag{3-77}$$

where ϕ_Q is the normalized σ_q. Again, experimental data in stable conditions present too large a scatter. But in unstable conditions

$$\phi_Q = const\ (z/L)^{-1/3} \tag{3-78}$$

with (Hogstrom and Hogstrom, 1974)

$$const = 1.04 \pm 0.13 \tag{3-79}$$

The above formulations have been successful only in flat terrain cases. Similar scaling approaches have been proposed for other layers in the PBL, but have not yet shown the same success.

3.7 SCALING IN OTHER LAYERS OF THE PBL

Parameterizations of the viscous sublayer near the ground (for $z < z_o$) have been proposed by Zilitinkevich (1970) and Deardorff (1974). Deardorff (1974) has also provided a parameterization of the mixing layer (from h_s to z_i), which seems very realistic when the variation of z_i with time is strongly influenced by surface heating (Pielke and Mahrer, 1975). Accordingly, σ_w can be scaled by

$$\sigma_w/w_* = f(z/z_i) \tag{3-80}$$

where the function f seems to be proportional to $(z/z_i)^{1/3}$.

Internal boundary layers are generated when air advects over heterogeneous surfaces. In these cases, at upper levels, turbulence is characteristic of the original surface, while, at lower levels, it is a function of the new surface. The interface between these two regimes (e.g., stable above and unstable below, or vice versa) is called the internal boundary layer. Deardorff and Peterson (1980) and Deardorff (1981) give a tentative parameterization of such horizontally non-homogeneous boundary layers. Further discussion of internal boundary layer phenomena is provided by Hunt and Simpson (1982).

New insight on the stable atmospheric boundary layer has recently been provided by the "local scaling" approach (Nieuwstadt, 1984), in which a local (i.e., variable with z) Obukhov length Λ is defined as

$$\Lambda(z) = \frac{\tau^{3/2}(z)}{k \frac{g}{T} \overline{w'\theta'}(z)} \tag{3-81}$$

where T is the temperature and w', θ' are the fluctuations of vertical wind velocity and potential temperature (see Section 3.5.8), respectively. The profiles $\tau(z)$, $\overline{w'\theta'}(z)$ and $\Lambda(z)$ can be expressed by the power laws

$$\tau(z)/\tau(0) = (1 - z/h)^{\alpha_1} \tag{3-82}$$

$$\overline{w'\theta'}(z)/\overline{w'\theta'}(0) = (1 - z/h)^{\alpha_2} \tag{3-83}$$

$$\Lambda(z)/L = (1 - z/h)^{\alpha_3} \tag{3-84}$$

where h is the mean mixing height.

The above scheme was not justified theoretically, but seems to provide a convenient approximation, even though it is in contradiction with local scaling

(Holtslag and Nieuwstadt, 1986). In spite of this problem, in horizontally homogeneous and steady conditions, Nieuwstadt (1984) derived $a_1 = 3/2$, $a_2 = 1$ and $a_3 = 5/4$.

Finally, the new "local similarity" theory by Sorbjan (1986 and 1988) must be mentioned. Sorbjan (1986) generalized the Monin–Obukhov (1954) similarity theory to the region above the surface layer and provided universal functions, in agreement with empirical data, for the stable and convective regimes. This extension of the similarity theory, however, is valid only in the lower half of the mixed layer. Sorbjan (1988) presented new hypotheses with new similarity functions that generalize local scaling for the entire mixed layer in convective (i.e., unstable) conditions.

REFERENCES

Aloysius, K.L. (1979): On the determination of boundary-layer parameters using velocity profile as the sole information. *Boundary-Layer Meteor.*, **17**:465–484.

Businger, J.A. (1966): Transfer of heat and momentum in the atmospheric layer. Prog. Artc. Heat Budget and Atmos. Circulation. Rand Corp., Santa Monica, California, pp. 305–332.

Businger, J.A., and S.P. Arya (1974): Heights of the mixed layer in the stable, stratified planetary boundary layer. *Advances in Geophys.*, **18A**:73–92.

Caughey, S.J., and S.G. Palmer (1979): Some aspects of turbulence structure through the depth of the convection boundary layer. *Quart. J. Roy. Meteor. Soc.*, **105**:811–827.

Caughey, S.J., J.C. Wyngaard, and J.C. Kaimal (1979): Turbulence in the evolving stable boundary layer. *J. Atmos. Sci.*, **36**:1041–1052.

Deardorff, J.W. (1970): Convective velocity and temperature scales for the unstable planetary boundary layer. *J. Atmos. Sci.*, **27**:1211–1213.

Deardorff, J.W. (1974): Three-dimensional numerical study of the height and mean structure of a heated planetary boundary layer. *Boundary-Layer Meteor.*, **7**:81–106.

Deardorff, J.W., and E.W. Peterson (1980): The boundary-layer growth equation with Reynolds averaging. *J. Atmos. Sci.*, **37**:1405–1409.

Deardorff, J.W. (1981): Further considerations on the Reynolds average of the kinematic boundary condition. *J. Atmos. Sci.*, **38**:659–661.

Dobbins, R.A. (1979): *Atmospheric Motion and Air Pollution*. New York: John Wiley.

Garratt, J.R. (1982): Observations in the nocturnal boundary layer. *Boundary-Layer Meteor.*, **22**(1):21–48.

Golder, D. (1972): Relations among stability parameters in the surface layer. *Boundary-Layer Meteor.*, **3**:47–58.

Gryning, S.E., A.A. Holtslag, J.S. Irwin, and B. Sivertsen (1987): Applied dispersion modelling based on meteorological scaling parameters. *Atmos. Environ.*, **21**(1):79–89.

Hogstrom, U., and A.S. Hogstrom (1974): Turbulence mechanism at an agricultural site. *Boundary-Layer Meteor.*, **7**:373–389.

Holtslag, A.A., and F.T. Nieuwstadt (1986): Scaling the atmospheric boundary layer. *Boundary-Layer Meteor.*, **36**:201–209.

Hunt, J.C., and J.E. Simpson (1982): Atmospheric boundary layers over nonhomogeneous terrain. In *Engineering Meteorology*, editted by E. Plate, New York: Elsevier, pp. 269–318.

Irwin, J.S. (1979): Estimating plume dispersion: A recommended generalized scheme. Presented at 4th AMS Symposium on Turbulence and Diffusion, Reno, Nevada.

Liu, M.-K., D.R. Durran, P. Mundkur, M. Yocke, and J. James (1976): The chemistry, dispersion, and transport of air pollutants emitted from fossil fuel plants in California: Data analysis and emission impact model. Final report to the Air Resources Board, Contract No. ARB 4-258, Sacramento, California.

McRae, G.J., W.R. Goodin, and J.H. Seinfeld (1982): Mathematical modeling of photochemical air pollution. EQL Report No. 18, Environmental Quality Laboratory, Pasadena, California. Also see: McRae, G.J., W.R. Goodin, and J.H. Seinfeld (1982): Development of a second generation mathematical model for urban air pollution, I. Model formulation. *Atmos. Environ.*, **16**(4):679–696.

Monin, A.S., and A.M. Obukhov (1954): Basic laws of turbulent mixing in the ground layer of the atmosphere. *Trans. Geophys. Inst. Akad.*, Nauk USSR **151**:163–187.

Nieuwstadt, F.T. (1978): The computation of the friction velocity u_* and the temperature scale T_* from temperature and wind velocity profiles by least-squares methods. *Boundary-Layer Meteor.*, **14**:235–246.

Nieuwstadt, F.T. (1984): The turbulent structure of the stable nocturnal boundary layer. *J. Atmos. Sci.*, **41**:2202–2216.

Pandolfo, J.O. (1966): Wind and temperature for constant flux boundary layers in lapse conditions with a variable eddy conductivity to eddy viscosity ratio. *J. Atmos. Sci.*, **23**:495–502.

Panofsky, H.A., H. Tennekes, D.H. Lenscfhow, and J.C. Wyngaard (1977a): The characteristics of turbulent velocity components in the surface layer under convective conditions. *Boundary-Layer Meteor.*, **11**:355–361.

Panofsky, H.A., W. Heck, and M.A. Bender (1977b): The effect of clear-air turbulence on a model of the general circulation of the atmosphere. *Beitr. Phys. Atmos.*, **50**:89–97.

Panofsky, H.A., and J.A. Dutton (1984): *Atmospheric Turbulence*. New York: John Wiley.

Pasquill, F. (1974): *Atmospheric Diffusion*, 2nd Edition. New York: Halsted Press of John Wiley & Sons.

Pielke, R.A., and Y. Mahrer (1975): Technique to represent the heated-planetary boundary layer in mesoscale models with coarse vertical resolution. *J. Atmos. Sci.*, **32**:2288–2308.

Pielke, R.A. (1984): *Mesoscale Meteorological Modeling*. Orlando, Florida: Academic Press.

Sorbjan, Z. (1986): On similarity in the atmospheric boundary layer. *Boundary-Layer Meteor.*, **34**:377–397.

Sorbjan, Z. (1988): Local similarity in the convection boundary layer (CBL). *Boundary-Layer Meteor.*, **45**:237–250.

Stern, A.C., R.W. Boubel, D.B. Turner, and D.L. Fox (1984): *Fundamentals of Air Pollution*. Orlando, Florida: Academic Press.

van Ulden, A.P., and A.A. Holtslag (1985): Estimation of atmospheric boundary layer parameters for diffusion applications. *J. Climate and Appl. Meteor.*, **24**:1196–1207.

Venkatram, A. (1980): Estimating the Monin-Obukhov length in the stable boundary layer for dispersion calculations. *Boundary-Layer Meteor.*, **19**:481–485.

Wilczak, J.M., and M.S. Phillips, (1986): An indirect estimation of convection boundary layer structure for use in pollution dispersion models. *J. Climate and Appl. Meteor.*, **25**:1609–1624.

Williamson, S.J. (1973): *Fundamentals of Air Pollution*. Reading, Massachusetts: Addison-Wesley.

Wyngaard, J.C., O.R. Cote, and K.S. Rao (1974): Modeling the atmospheric boundary layer. *Advances in Geophys.*, **18A**:193–211.

Wyngaard, J.C., and M.A. LeMone (1980): Behavior of the refractive index structure parameter in the entraining convective boundary layer. *J. Atmos. Sci.*, **37**:1573–1585.

Zilitinkevich, S.S. (1970): *Dynamics of the Atmospheric Boundary Layer*. Leningrad: Hydrometerol.